Active-sterile neutrino mixing constraints using reactor antineutrinos with the ISMRAN setup

S. P. Behera,* D. K. Mishra, and L. M. Pant

Nuclear Physics Division, Bhabha Atomic Research Centre, Mumbai-400085, India

(Received 11 February 2020; accepted 30 June 2020; published 10 July 2020)

In this work, we present an analysis of the sensitivity to the active-sterile neutrino mixing with the Indian Scintillator Matrix for Reactor Anti-Neutrino (ISMRAN) experimental setup at very short baseline. The 3 (active) + 1 (sterile) neutrino oscillation model is considered to study the sensitivity of the active-sterile neutrino in the mass splitting and mixing angle plane. In this article, we have considered the measurement of electron antineutrino induced events employing a single detector which can be placed either at a single position or moved between a near and far positions from the given reactor core. Results extracted in the later case are independent of the theoretical prediction of the reactor anti-neutrino spectrum and detector related systematic uncertainties. Our analysis shows that the results obtained from the measurement carried out at combination of the near and far detector positions are improved significantly at higher Δm^2_{41} compared to the ones obtained with the measurement at a single detector position only. It is found that the best possible combination of near and far detector positions from a 100 MW_{th} power DHRUVA research reactor core are 7 m and 9 m, respectively, for which ISMRAN setup can exclude in the range 1.4 $eV^2 \leq \Delta m^2_{41} \leq 4.0$ eV^2 of reactor antineutrino anomaly region along with the present best-fit point of active-sterile neutrino oscillation parameters. At those combinations of detector positions, the ISMRAN setup can observe the active sterile neutrino oscillation with a 95% confidence level provided that $\sin^2 2\theta_{14} \geq 0.09$ at $\Delta m^2_{41} = 1$ eV^2 for an exposure of 1 ton-yr. The active-sterile neutrino mixing sensitivity can be improved by about 22% at the same exposure by placing the detector at near and far distances of 15 m and 17 m, respectively, from the compact proto-type fast breeder reactor (PFBR) facility which has a higher thermal power of 1250 MW_{th}.

DOI: 10.1103/PhysRevD.102.013002

I. INTRODUCTION

Nuclear reactors are a copious source of electron antineutrinos due to beta decay of neutron-rich fission products. About 6 electron antineutrinos ($\bar{\nu}_e$) are produced per fission, corresponding to $\sim 10^{20}$ antineutrinos per second from a reactor of thermal power 1 GW_{th}. Electron antineutrinos produced from the reactors played important roles in the history of particle physics, from establishing the existence of neutrinos [1] to determining the nonzero value of mixing angle (θ_{13}) by Double Chooz [2], Daya Bay [3], and RENO [4] experiments. These experiments used near and far detector(s) to cancel out correlated systematic uncertainties due to the reactor $\bar{\nu}_e$ flux and the dependence on the absolute flux and thus have significantly improved precision measurement of θ_{13} over single detector experiments.

Observations of the reactor $\bar{\nu}_e$ flux suffer an anomalous and unexplained behavior. The theoretical calculation of the $\bar{\nu}_e$ flux by Mueller *et al.* [5] and Huber [6] predicts 6% more events than those observed in several reactor experiments at small distances. This is known as the "reactor antineutrino anomaly" (RAA) [7]. The source of this anomaly is not known yet. However, there are two possible proposed explanations for this discrepancy. One of them is an incomplete prediction of the antineutrino flux and energy spectrum from reactors, due to underestimated systematics of the measurements of beta spectra emitted after fission [8–10] or of the conversion method [5,6,11,12]. The other explanation is the disappearance of $\bar{\nu}_e$s while propagating from the source to detector due to active-sterile neutrino oscillations with mass squared difference ~ 1 eV^2. In addition, there can be a third possible explanation represented by possible unknown processes that affect the measurements.

The measurement of the reactor $\bar{\nu}_e$ induced positron spectra shows a statistically significant excess of events over the prediction, particularly in the energy spectrum at the range of 5–7 MeV (the so-called reactor bump). It puts

*shiba@barc.gov.in

in question the correctness of the flux calculation or to explore explanations with a new physics. An excess of events in the $\bar{\nu}_e$ spectra is observed by Double Chooz [13], Daya Bay [14], and RENO [15] Collaborations as well as other short baseline experiments such as NEOS [16]. The bump in energy spectra has been correlated to the power of the reactor [14], and may be due to the ^{235}U fuel [17]. To verify the hypothesis of the existence of active to sterile neutrino oscillation as a possible origin of the RAA, as well as to clarify the origin of the bump at 5 MeV in the $\bar{\nu}_e$ spectra at a very significant confidence level, several experiments are currently underway and will collect data soon [18].

To address the RAA, the short-baseline (SBL) experiments are aiming to measure the reactor antineutrino energy spectra at two or more different distances and are trying to reconstruct the $\bar{\nu}_e$s survival probability both as a function of energy and the source to detector distance, L. The measurement of data at two distances with respect to the measurement at a single position is less sensitive to the modification of the $\bar{\nu}_e$ spectra due to the time evolution of fuel composition in the reactor core, known as the burn-up effect, which is a source of systematic uncertainty. The L dependence is what gives the cleanest signal in the case of the sterile neutrino, and studying the ratio of the spectra measured at two different distances allows to avoid almost completely the problem of the theoretical spectrum. Based on this approach, several experiments have collected data to study the active-sterile neutrino oscillation. The DANSS collaboration [19] has measured the positron energy spectra at 3 different distances from the reactor core. The distances were varied from 10.7 m to 12 m to observe the active-sterile neutrino oscillations. Their observation excludes a large fraction of RAA region in the $\sin^2 2\theta_{14} - \Delta m^2_{41}$ plane and covers the parameter space up to $\sin^2 2\theta_{14} < 0.01$. The STEREO [20] collaboration has measured the antineutrino energy spectrum in six different detector cells covering baselines between 9 and 11 meters from the core of the ILL research reactor. The results based on the reactor ON data are compatible with the null active-sterile neutrino oscillation hypothesis and the best-fit of the RAA can be excluded at 97.5% confidence level (C.L.). The PROSPECT collaboration has measured the reactor $\bar{\nu}_e$ spectra using a movable segmented detector array. Their observation disfavors the RAA best-fit point at 2.2σ C.L. and constrains a significant portion of the previously allowed parameter space at 95% C.L.[21]. The Neutrino-4 experiment has measured $\bar{\nu}_e$ energy spectra by mounting the segmented detector on a movable platform which covers a baseline range from 6 to 12 meters. Their model-independent analysis excludes the RAA region at C.L. more than 3σ. However, the experiment has observed active-sterile neutrino oscillation at $\sin^2 2\theta_{14} = 0.39$ and $\Delta m^2_{41} = 7.3$ eV^2 at C.L. of 2.8σ [22]. The Neutrino-4 best-fit is incompatible with PROSPECT bounds. To this end, the Indian Scintillator Matrix for Reactor Anti-Neutrino (ISMRAN) detector is proposed. It will be mounted on a movable trolley in order to place the complete setup at different distances with respect to the reactor core. Here we study its potential to observe active-sterile neutrino oscillation at SBL ($L < 25$ m). An investigation is carried out employing the $3 + 1$ neutrino mixing model, where "3" refers to active neutrinos and "1" to sterile neutrinos. This is the only allowed active-sterile neutrino mixing scheme [23] under the assumption of 4 neutrino model. The existence of active-sterile neutrino oscillation with mass squared difference $\Delta m^2_{41} (= m^2_4 - m^2_1) \sim 1$ eV^2 can be explored at the SBL experiment by measuring the reactor $\bar{\nu}_e$ flux which is reduced due to the fast active to sterile neutrino oscillation that is otherwise absent in the 3-neutrino mixing scheme. A similar study has been performed previously, considering a single detector which will be placed at a fixed distance from the reactor core by varying both reactor and detector related parameters [24]. To reduce the systematic uncertainties mentioned earlier, in this work we have considered various possible combinations of near and far positions for the same 1-ton detector which will be placed for a period of six months at each distance while constraining active-sterile neutrino oscillation parameters. It can be noted that, in case of a research reactor the burn-up period is small and the time evolution of fuel has less impact on the modification of $\bar{\nu}_e$ spectra. Hence, we can either place it six months at each location or shift the position of the detector more frequently. On the other hand, a power reactor has a longer burn-up period. Therefore, it is important to consider the fuel evolution of the reactor with time, which can be minimized by changing the position of the detector more frequently.

The article is organized in the following order. A detailed description of the ISMRAN setup and neutrino detection principle is discussed in Sec. II and Sec. III, respectively. The phenomenon of active-sterile neutrino oscillation at SBL considering the '$3 + 1$' mixing model is described in Sec. IV. The procedure for the incorporation of detector response on $\bar{\nu}_e$ induced simulated events is mentioned in Sec. V. In order to find out the ISMRAN setup sensitivity to the active-sterile neutrino oscillation parameters, a statistical method on χ^2 estimation considered in this study is discussed in Sec. VI. The sensitivity to active-sterile neutrino mixing at an exposure of 1 ton-yr is elaborated in Sec. VII. In Sec. VIII, we summarize our observations and discuss the implication of this work.

II. THE ISMRAN SETUP

The one-ton active volume ISMRAN setup consists of 100 segmented plastic scintillator (PS) bars with a total volume of 1 m^3. The size of each PS bar is 100 cm $\times$ 10 cm $\times$ 10 cm and is wrapped with aluminized mylar foils that have been coated with gadolinium. The gadolinium coating increases the detection efficiency of neutrons. At

both ends, a PS bar is coupled with two 3 inch photomultiplier tubes. More information on the detector and background measurements carried out at the experimental site can be found in Ref. [25]. Due to the compact size of the detector, it can be easily maneuvered from one place to another. This is useful for the remote monitoring of the power of the reactor. The segmented detectors array can provide additional position information while reconstructing the neutrino induced events and thus will improve the active sterile neutrino mixing sensitivity of the ISMRAN setup. The energy and position information of an event will be extracted from the signals of the PS bars. All signals will be digitized with a CAEN-made digitizer. Details of the signal processing and data acquisition are given in Ref. [25]. The ISMRAN setup active volume is surrounded with passive shielding material consisting of 10 cm thick Lead followed by 10 cm thick borated polyethylene in order to suppress both the natural and reactor related background such as gamma-rays and neutrons. Further, the setup will be surrounded by 1-inch thick scintillator plates for vetoing the cosmic muons.

The proposed ISMRAN setup will be placed at the DHRUVA research reactor facility in Bhabha Atomic Research Centre (BARC), India. The setup consists of inflammable plastic scintillator detectors, so they can be placed as close as possible to the reactor core. The closest possible distance at which the detector can be placed is about 7 m from the reactor core. The DHRUVA reactor core has a cylindrical shape with radius ∼1.5 m and height ∼3.03 m (defined as an extended source) [26]. The reactor can operate at a maximum thermal power of 100 MW_{th} consuming natural uranium as fuel. In the future, it is planned to put the ISMRAN setup at other reactor facilities such as upgraded Apsra (U-Apsra) reactor [27], BARC, and, proto-type fast breeder reactor (PFBR), IGCAR, Kalpakkam, India [28].

The U-Apsra reactor has a compact core with a height of about 0.64 m and radius about 0.32 m which can operate at a maximum thermal power of 3 MW_{th} [27]. The closest possible distance at which the detector can be placed is about 4 m from the reactor core, which is an ideal position considering average $\bar{\nu}_e$ energy about 4 MeV and active-sterile neutrino oscillation at $\Delta m^2_{41} \simeq 1$ eV^2. At this distance, L/E value is of the order of 1 m/MeV. Hence, this will maximize the sensitivity to sterile neutrino masses at the eV-scale. On the other hand, PFBR is a relatively compact source with respect to DHRUVA reactor. The PFBR has dimensions of about 1 m in both radius and height. The PFBR can operate at a maximum thermal power of 1250 MW_{th} and employs mixed oxide (MOX, PuO_2-UO_2) as fuel [28]. The closest possible distance at which the detector can be placed is about 15 m from PFBR core. These compact U-Apsra and PFBR reactors are ideal sources to utilize the ISMRAN setup for investigating the active-sterile neutrino mixing at a short distance. However, at such close distances, there are significant contributions from the reactor related background on the sterile neutrino sensitivity. At present, measurements of reactor related backgrounds are going on with a proto-type ISMRAN setup consists of 16 PS bars placed at a distance of 13 m from DHRUVA reactor core. The above-mentioned reactors are not only different in terms of their sizes and thermal power but also different with respect to their various fuel compositions as mentioned in Table I. These reactors have different fuel compositions and hence the measurements with ISMRAN setup will be different from existing worldwide experimental observations because of the different $\bar{\nu}_e$ fluxes at each reactor. This will be an ideal situation to compare with other results regarding the bump at 5 MeV.

TABLE I. Reactor details.

Reactors name	Thermal power (MW_{th})	Fuel type
DHRUVA	100.0	Natural uranium
PFBR	1250.0	MOX(PuO_2-UO_2)
U-Apsra	3.0	U_3Si_2-Al (Low enriched ^{235}U)

III. THE $\bar{\nu}_e$ DETECTION PRINCIPLE

The PS bars in the ISMRAN setup act as a target as well as active detection material for the $\bar{\nu}_e$s. The basic principle of detection for $\bar{\nu}_e$s produced from the reactors is via the inverse beta decay (IBD) process. The IBD process is given by

$$\bar{\nu}_e + p \rightarrow n + e^+. \quad (1)$$

The minimum antineutrino energy required for the above reaction to occurs is about 1.80 MeV. In this process, the positron carries almost all of the available energy, loses it by ionization in the detector, and produces two γ-rays each having energy 0.511 MeV through annihilation process. This is the "prompt" signal. The neutron produced through the IBD process carries a few keV's of energy and gets thermalized within several μs in collisions with protons in the PS bar. The thermal neutron then gets captured by hydrogen (captured time of ∼200 μs) in the PS bar. This is the "delayed" signal. In this case, a monoenergetic gamma-ray of energy 2.2 MeV is produced, comparable to the gamma-ray energy originated from some of the natural backgrounds. To further increase the probability for neutron capture and improve the detection efficiency, PS bars are wrapped with gadolinium (Gd) coated aluminized mylar foil as both ^{155}Gd and ^{157}Gd have high thermal neutron capture cross section. Hence, the reduced neutron capture time is ∼60 μs, observed in prototype ISMRAN setup [25]. There is also a cascade of gamma-rays produced with a total energy of about 8 MeV due to neutrons captured in the gadolinium. Due to higher total energy, it is possible to distinguish these gamma-rays from the

natural background. The coincidence of a prompt positron signal and a delayed signal from captured neutron uniquely identifies the IBD event.

The detection of candidate events is dominated by two types of backgrounds. The first is the accidental background as a result of two random energy depositions in a time window corresponding to the captured time of the neutron. The other type of background is the correlated background originating from either spallation of cosmic muons, which produces fast neutrons, or fast neutrons coming from the reactor due to fission fragments. The prompt signal arises due to the energy loss of fast neutrons through scattering off protons and a delayed signal due to captured neutron in PS, both constitute a IBD-like event. However, efficient delayed coincidence technique allows us to suppress such types of backgrounds [29]. These background contributions would affect the detector sensitivity, so it is essential to reduce them. This is discussed further in Sec. VII.

IV. NEUTRINO OSCILLATION PROBABILITY AT SHORT BASE LINE

There are three flavors of active neutrinos (ν_e, ν_μ, ν_τ) in the standard model. Neutrinos are produced and detected as flavor states. However, they propagate as superpositions of mass eigenstates. The transformation between flavor and mass eigenstates is expressed by the Pontecorvo-Maki-Nakagawa-Sakata (PMNS) [30] unitary matrix. The establishment of phenomena of neutrino oscillation and measurements of the three generations of oscillation parameters are carried out by several experiments [31–34]. At present, various experiments are aiming to measure the oscillation parameters more precisely. However, beyond these three active neutrinos, world-wide research programs are underway and some experiments will take data in the near future to explore the possible existence of active-sterile neutrino oscillation. The active-sterile neutrino mixing sensitivity of the ISMRAN setup is studied considering the "3 + 1" neutrino mixing model which was mentioned earlier. In this model, the 3 generation PMNS matrix are expanded to the 3 + 1 generation, where "3" stands for three active neutrinos and "1" for a sterile neutrino (ν_s). The order of rotation and elements of the mixing matrix are given in Ref. [24]. At a small value of mixing angle θ_{14} and source to detector distance of few meters (< 100 m), the 3 + 1 oscillation scheme can be simplified to a two neutrino scheme and the ν survival probability is approximated to

$$P_{\nu_e\nu_e}(E_\nu, L) \simeq 1 - \sin^2 2\theta_{14} \sin^2\left(\frac{1.27\Delta m^2_{41} L}{E_\nu}\right), \quad (2)$$

where E_ν is the neutrino energy (in MeV), L is the distance (in m) between the production and the detection of the neutrino and Δm^2_{41} is the squared masses difference (in eV^2) between the two neutrino mass eigenstates. The oscillation parameters Δm^2_{41} and $\sin^2 2\theta_{14}$ are given by

$$\Delta m^2_{41} = m^2_4 - m^2_1; \qquad \sin^2 2\theta_{14} = 4|U_{e4}|^2(1 - |U_{e4}|^2), \quad (3)$$

where U_{e4} is an element of the unitary mixing matrix. The oscillation probabilities for antineutrinos can be obtained by replacing the mixing matrix elements Us with their complex conjugate ($U*$s). However, at SBL experiments, the oscillation probability is independent of the CP-violating phases [35]. Hence the oscillation probability given in Eq. (2) is the same for antineutrino. Experimental studies on neutrino oscillations aim to determine the mass parameter Δm^2_{41} and the mixing angle $\sin^2 2\theta_{14}$. These parameters can be obtained by measuring the neutrino flux at different energies and distances. The present best-fit values of active-sterile neutrino oscillation parameters are $\Delta m^2_{41} \simeq 1.30$ eV^2 and $\sin^2 2\theta_{14} \simeq 0.049$ [36] extracted from the combined analysis of data taken by NEOS and DANSS collaborations. Similar values are also found from global analysis [37]. At these values of the neutrino oscillation parameters, the possible existence of sterile neutrino at SBL experiments can be observed by looking at the distortions of the $\bar{\nu}_e$ energy spectrum at short distances which are otherwise absent in the three active neutrino oscillations. However, these distortions are smeared out for longer source to detector distances and the phase factor of the oscillation probability averaged out to $1/2$. This leads to the survival probability of $1 - \sin^2 2\theta_{14}/2$. Hence, we lose the information regarding Δm^2_{41} and can measure only the mixing angle θ_{14}. However, measuring the oscillation parameters by measuring $\bar{\nu}_e$s with a detector placed at only one distance from the reactor core and comparing it with the prediction is not enough, since the theoretical calculation of the $\bar{\nu}_e$ energy distribution is not reliable enough. Therefore, the most reliable way to observe such distortions is to measure the $\bar{\nu}_e$ spectrum with the same detector at various distances. In this case, the shape and normalization of the $\bar{\nu}_e$ spectrum as well as the detector efficiency are canceled out. Alternatively, one can put two same types of detectors at near and far positions in order to avoid the assumption of constant reactor flux. In such a case, although two detectors of the same type, their response and other detector related parameters may not be the same, which will introduce the detector related uncertainties.

V. SIMULATION PROCEDURE

The potential of the ISMRAN setup on finding active-sterile neutrino oscillation sensitivity will be explored by using antineutrinos produced from various types of reactor facilities such as the U-Apsra, DHRUVA, and PFBR. The number of $\bar{\nu}_e$s produced from the reactor not only depends on the thermal power but also on their fuel compositions. The energy spectrum of the $\bar{\nu}_e$s produced from the reactor is different for different isotopes. The parametrization for $\bar{\nu}_e$ flux assumed in the present analysis is as follows:

TABLE II. Fractional contributions of each element to the reactor thermal power and the parameters used to fit the neutrino spectrum.

Element	a			b_0	b_1	b_2	b_3	b_4	b_5
	U-Apsra	DHRUVA	PFBR						
^{235}U	0.90	0.58	0.0093	4.367	−4.577	2.1	−0.5294	0.06186	−0.002777
^{239}Pu	0.07	0.30	0.71	4.757	−5.392	2.63	−0.6596	0.0782	−0.003536
^{241}Pu	0.01	0.05	0.11	2.99	−2.882	1.278	−0.3343	0.03905	−0.001754
^{238}U	0.02	0.07	0.10	0.4833	0.1927	−0.1283	−0.006762	0.002233	−0.0001536

$$f(E_{\bar{\nu}_e}) = \sum_{i=0}^{4} a_i \exp\left(\sum_{j=0}^{6} b_j E_{\bar{\nu}_e}^{j-1}\right), \quad (4)$$

where "a_i" is the fractional contribution from the ith isotope to the reactor thermal power, "b_j's" are the constant terms used to fit the antineutrino energy spectra, and $E_{\bar{\nu}_e}$ is neutrino energy in MeV. The fractional contributions of each isotope to the reactor thermal power and the parameter lists used to fit the neutrino energy spectra are summarized in Table II. Both a_i and b_j values for various isotopes are taken from Ref. [38] and Ref. [39] for the DHRUVA and PFBR reactors, respectively. In the case of the U-Apsra reactor, we have assumed the fractional contributions of each isotope to the reactor thermal power as mentioned in Table II. The list of parameters used to fit the $\bar{\nu}_e$ spectra due to ^{235}U, ^{239}Pu, and ^{241}Pu are considered from Ref. [6] and for ^{238}U is taken from Ref. [5]. We have also considered the spatial variation of $\bar{\nu}_e$ flux due to a finite size cylindrical reactor that depends on the radius and height of the core which is given by [40],

$$\phi = \phi_0 J_0(2.405r/R)\cos(\pi z/H) \quad (5)$$

where ϕ_0 represents the flux at the center of the reactor core, R is the radius of the cylindrical reactor core, H is the height, J_0 is the zeroth-order Bessel function of the first kind where r $(0 \le r \le R)$ and z $(0 \le z \le H)$ are the vertex positions of the $\bar{\nu}_e$s produced in the reactor. The interaction cross section of $\bar{\nu}_e$ for the inverse IBD process is given by [41]

$$\sigma_{\mathrm{IBD}} = 0.0952 \times 10^{-42}\ \mathrm{cm}^2 (E_{e^+} p_{e^+}/\mathrm{MeV}^2), \quad (6)$$

where $E_{e^+} = E_{\bar{\nu}_e} - (m_n - m_p)$ is the positron energy, neglecting the recoil neutron kinetic energy, and p_{e^+} is the positron momentum. The detector resolution is folded on the true positron (kinetic) energy spectrum by assuming a standard Gaussian form of the energy resolution:

$$R(E_{e^+}, E_{e^+,T}) = \frac{1}{\sqrt{2\pi}\sigma}\exp\left(-\frac{(E_{e^+} - E_{e^+,T})^2}{2\sigma^2}\right) \quad (7)$$

where $E_{e^+,T}$ and E_{e^+} are the simulated true and observed positron energy, respectively. The detector resolution considered for this study is in the form $\sigma/E_{e^+} \sim 20\%/\sqrt{E_{e^+}}$. The neutrino induced events are distributed in terms of positron energy spectrum. There are a total of 80 bins in the e^+ energy range of 0–8 MeV that are considered. The number of events in ith energy bin after incorporating the detector resolution is given as

$$N_i^r = \sum_k K_i^k (E_{e^+,T}^k) n_k. \quad (8)$$

The index i corresponds to the measured energy bin, N_i^r corresponds to the number of reconstructed events, k is summed over the true energy of positron and n_k is the number of events in kth true energy bin. Further, K_i^k is the integral of the detector resolution function over the E_{e^+} bins and is given by

$$K_i^k = \int_{E_{e^+,L_i}}^{E_{e^+,H_i}} R(E_{e^+}, E_{e^+,T}) dE_{e^+} \quad (9)$$

The integration is performed between the lower and upper boundaries of the measured energy (E_{e^+,L_i} and E_{e^+,H_i}) bins. In the present analysis, we have assumed 25% detection efficiency, 80% fiducial volume of the detector, and 70% reactor duty cycle for an exposure of 1 ton-year. Both the production point of neutrinos in the reactor core and the interaction point in the detector are generated using a Monte-Carlo method.

VI. SENSITIVITY ESTIMATION

The active-sterile neutrino mixing sensitivity of an experiment can be extracted by two independent pieces of information. The first is by knowing the $\bar{\nu}_e$ energy spectrum, flux, and cross section accurately. From this, the total number of $\bar{\nu}_e$ induced events expected within the detector can be estimated for a given oscillation hypothesis and compared with the measured one. This is known as a "rate only" analysis. The second case is a relative change of event rate as a function of the source to detector distance and $\bar{\nu}_e$ energy that can be compared with the predictions taking different oscillation hypotheses, without constraining the integral number of events. Using this method to find the sensitivity of the oscillation parameters is known as "shape only" analysis. A combination of rate only and

shape only analyses are used (known as "rate + shape" analysis) in order to maximize the experimental sensitivity. These methods are affected by different systematic uncertainties.

A statistical analysis of simulated event distribution for an exposure of 1 ton-year is performed in order to quantify the sensitivity of ISMRAN setup to the active-sterile neutrino mixing parameters θ_{14} and Δm^2_{41}. The detector response is incorporated in both theoretically predicted (events without active-sterile neutrino oscillation) and number of events expected due to active-sterile neutrino oscillation. The exclusion limit is extracted by estimating the χ^2 for each value of Δm^2_{41} with scanning over the various values of $\sin^2 2\theta_{14}$, and determining the boundary of the corresponding χ^2 [e.g., $\chi^2 = 5.99$ for 95% confidence limit(C.L.)]. Based on the "rate + shape" analysis, the definition of χ^2 is taken from Ref. [42] and is given by

$$\chi^2 = \sum_{n=0}^{N} \left(\frac{N_n^{\text{th}} - N_n^{\text{ex}}}{\sigma(N_n^{\text{ex}})} \right)^2 + \sum_{i=0}^{k} \xi_i^2 \tag{10}$$

where n is the number of energy bins, N_n^{ex} is the expected number of observed events (with oscillations), and N_n^{th} is the number of theoretically predicted events (without oscillations). The theoretically predicted events, N_n^{th} are calculated considering reactor antineutrino flux as given by the Huber and Mueller model mentioned in Eq. (4), the IBD cross section, the detection efficiency, and detector energy resolutions. The simulated oscillated event, N_n^{ex} is estimated by folding the oscillation probability on N_n^{th}. N_n^{th} carries the information about systematic uncertainties given by

$$N_n^{\text{th}} = N_n'^{\text{th}} \left(1 + \sum_{i=0}^{k} \pi_n^i \xi_i \right) + \mathcal{O}(\xi^2) \tag{11}$$

where $N_n'^{\text{th}}$ is the theoretically predicted event spectrum given by Eq. (8). In the above π_n^i is the strength of the coupling between the pull variable ξ_i and $N_n'^{\text{th}}$. The χ^2 is minimized with respect to pull variables ξ_i. The index i in Eqs. (10) and (11) runs from 0 to k, where k is the total number of systematic uncertainties. We have considered four systematic uncertainties in our analysis. These include 3% normalization uncertainty (including reactor total neutrino flux, number of target protons, and detector efficiency), a nonlinear energy response of the detector by 1%, and, uncertainty in the energy calibration by 0.5%. The uncorrelated experimental bin-to-bin systematic error of 2%, which could occur due to insufficient knowledge of a source of background [43], is also considered. The definition given in Eq. (10) includes both the rate and spectral shape information of neutrino induced events.

In the case of "rate only" analysis, the χ^2 is estimated by integrating over energies as a single bin and setting all the systematic uncertainties to zero except the normalization uncertainty. It can be noted that the rate only analysis is sensitive to the active-sterile neutrino mixing angle. The "shape only" analysis is carried out considering the spectral shape information by setting the penalty term due to total reactor neutrino flux to zero. In this method, the oscillation frequency of Δm^2_{41} from the energy dependent disappearance of the reactor $\bar{\nu}_e$ is considered without using the information on the total-rate deficit. In the present analysis, we have studied the sensitivity of the detector considering shape only, rate only as well as combined rate + shape analysis separately, and compared the results obtained from each method.

Since there is ~6% uncertainty in the theoretical prediction of reactor neutrino flux, it is essential either to build two identical detectors and locate one at near site and the other at far site or a single detector placed for some previously established time periods at the near and far position for certain periods in order to measure the active-sterile neutrino oscillation parameters precisely. However, we have considered various possible combinations near and far positions of the same detector to reduce the systematic uncertainties. For the two detectors case, the chi-square is defined as follows [44],

$$\chi^2 = \sum_{n=0}^{N} \left(\frac{O_n^{F/N} - T_n^{F/N}}{\sigma(O_n^{F/N})} \right)^2, \tag{12}$$

where $O_n^{F/N}$ is the simulated far-to-near ratio of oscillated events in nth energy bin, $T_n^{F/N}$ is the expected far-to-near ratio of without oscillated events, and $\sigma(O_n^{F/N})$ is the statistical uncertainty of the oscillated event ratio $O_n^{F/N}$. It can be noted here that we have only considered the event spectra which will be measured at different far to near distances. The above definition of χ^2 does not depend on the exact knowledge of the reactor power, absolute $\bar{\nu}_e$ flux, burn up effects, and detector related uncertainties. The definition of chi-square given in Eq. (12) is modified while considering the background for both the far and near detectors which is as follows,

$$\chi^2_{\text{bkg}} = \sum_{n=0}^{N} \left(\frac{O_n^{F/N} - T_n'^{F/N}}{\sigma(O_n^{F/N})} \right)^2 + \sum_{d=N,F} \xi_d^2, \tag{13}$$

where $T_n'^{F/N}$ is defined as

$$T_n'^{F/N} = T_n^{F/N} \left(1 + \sum_{d=N,F} \pi_n^d \xi_{d.} \right) + \mathcal{O}(\xi^2) \tag{14}$$

In Eq. (14), π_n^d is the strength of the coupling between the pull variable ξ_d and $T_n^{F/N}$. The index d in Eqs. (13) and (14) is for the near and far detectors. The background

uncertainty is assumed to be 10.0% and 6.0% for near and far detectors, respectively.

VII. RESULTS AND DISCUSSIONS

A study on active-sterile neutrino mixing sensitivity has been performed previously with the ISMRAN setup placed at a fixed distance from the reactor core while varying both the reactor and detector related parameters [24]. In the present study, we have considered the system in which the measurement will be carried out by placing the same detector at multiple positions with respect to the reactor core in order to cancel out the systematic uncertainties. The detector sensitivities to active-sterile oscillation parameters are compared by measuring the $\bar{\nu}_e$s produced from various types of reactors which are mentioned in Table I.

A. Detector at fixed distance

Figure 1 shows the active-sterile neutrino oscillation sensitivity of ISMRAN setup in the $\sin^2 2\theta_{14} - \Delta m^2_{41}$ plane at 95% C.L. for an exposure of 1 ton-yr. The left, middle, and right panels represent the results by placing the single detector at 4 m, 13 m, and, 20 m distances from the U-Apsra, DHRUVA, and PBFR reactor cores, respectively. The dashed-dotted blue, dashed red, and solid green lines, respectively, show the sensitivity by performing the rate only, shape only, and a combination of rate + shape analysis.

In the case of the ISMRAN setup at the U-Apsra reactor facility, the shape of the sensitivity curve at low Δm^2_{41} (e.g., $0.1 \lesssim \Delta m^2_{41}\ (\mathrm{eV}^2) \lesssim 0.6$) region shows a linear dependence between $\sin^2 2\theta_{14}$ and Δm^2_{41} in a logarithmic scale. This is because the typical neutrino oscillation lengths are much larger compared to the size of the detector. Hence, the $\bar{\nu}_e$ survival probability mentioned in Eq. (2) approximates to $P_{\bar{\nu}_e\bar{\nu}_e}(E_{\bar{\nu}_e}, L) \approx 1 - C \sin^2 2\theta_{14} \times (\Delta m^2_{41})^2$, where C is a constant. It is observed that the shape only analysis has poor sensitivity to the oscillation parameters in the range $0.3 < \Delta m^2_{41}\ (\mathrm{eV}^2) < 1.5$ and for $\Delta m^2_{41} > 3.0\ \mathrm{eV}^2$ as compared to both rate only and rate + shape analysis. In the lower Δm^2_{41} region, the shapes of the flux distributions are poorly affected by the oscillation deformations, as oscillations do not have enough space to fully develop. In the higher Δm^2_{41} region, systematic uncertainties due to the antineutrino source dominate over statistical uncertainties. Also at higher Δm^2_{41}, the high-frequency oscillation probability gets averaged out due to the detector energy resolution. Both factors mentioned above result in a gradual decrease of the shape discriminating power. In the parameter range $\Delta m^2_{41} \sim 0.6$–$1.3\ \mathrm{eV}^2$, the ISMRAN setup has a maximum sensitivity with rate only and rate + shape analysis shown in left-panel of Fig. 1. It is found that results from both 'rate only' and 'rate + shape' analysis overlap for $\Delta m^2_{41} \geq 5.0\ \mathrm{eV}^2$. In this regime, the oscillation frequencies are large, and oscillations are suppressed by the detector energy resolutions and distribution of antineutrino path lengths. In case of rate + shape analysis, the rate deficit can be used to infer the $\sin^2 2\theta_{14}$ mixing parameter, leading to contours that do not depend on the squared mass splitting Δm^2_{41}. It has been concluded from the above study that rate + shape analysis procedure has the best sensitivity to the oscillation parameters as compared to both rate only and shape only analyses. The dotted magenta line shows the sensitivity due to rate + shape analysis for an exposure of 2 ton-yr. It shows an overall improvement in active-sterile neutrino mixing sensitivity due to the increase in statistics.

A similar behavior has been observed in the active-sterile neutrino mixing sensitivity of the detector using various analysis methods as mentioned above by considering the neutrino produced from DHRUVA and PFBR reactors. From this study, it is observed that the ISMRAN setup can exclude a small portion of RAA using the rate + shape analysis. In the above study, estimation of the sensitivity of

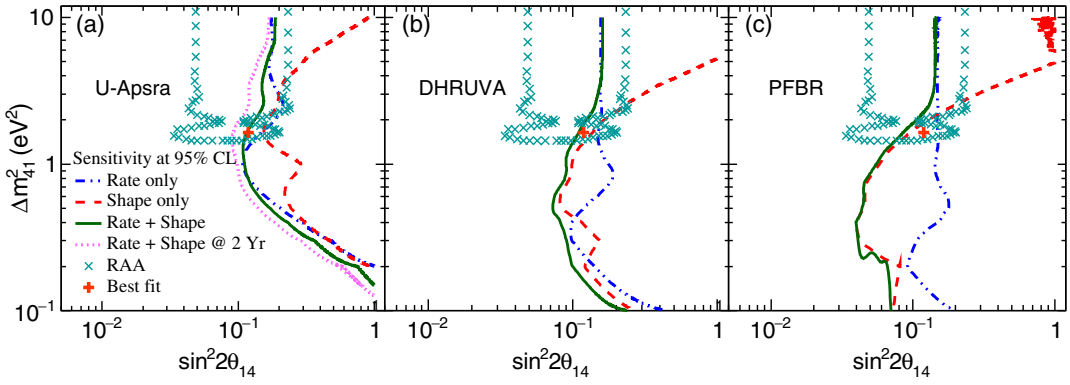

FIG. 1. The expected active-sterile neutrino mixing sensitivity of ISMRAN setup in the $\sin^2\theta_{14} - \Delta m^2_{41}$ plane. The left panel shows when the detector is placed at 4 m from the U-Apsra reactor core, the middle panel shows the case where the detector is positioned at 13 m from DHRUVA reactor core, and the right panel represents the study for which detector is placed at distance of 20 m from PFBR reactor core.

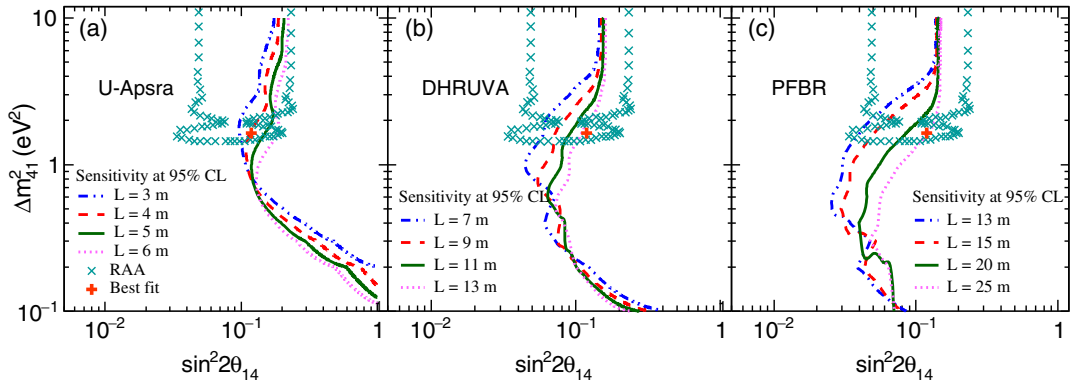

FIG. 2. The comparison of the expected active-sterile neutrino mixing sensitivity for the ISMRAN setup placed at different source to detector path lengths for the U-Apsra (left panel), DHRUVA (middle panel), and PFBR (right panel) reactors.

ISMRAN is done by considering various reactor core sizes as well as path lengths from source to detector. It is found that the detector has the best sensitivity to the oscillation parameters for a compact core compared to an extended one, due to the large uncertainty in path lengths in the later. It can be noted here that rest of our study has been carried out considering the rate + shape analysis method.

Figure 2 shows the active-sterile neutrino sensitivity of the detector at various distances from the reactor cores to the center of the detector. In our calculation, both antineutrino vertices and their interaction in the detector are generated randomly using the MC method which was mentioned earlier. At lower Δm^2_{41} ($\simeq$0.1 eV^2), the detector has the best sensitivity to the oscillation parameters by carrying out the measurements at the PFBR facility, due to high thermal power and relatively compact core. It is observed that the detector sensitivity improves with reducing the distance for higher Δm^2_{41} (> 1.0 eV^2). By reducing the distance from the reactor, the event statistics are increased and hence the experimental sensitivity. However, it is important to consider other shielding material structures surrounding the reactor core and associated reactor backgrounds while moving closer to the source.

Furthermore, the active-sterile neutrino sensitivity of the detector has been studied with and without the inclusion of background for three different types of reactors. Figure 3(a) shows the detector sensitivity in the $\sin^2\theta_{14} - \Delta m^2_{41}$ plane without inclusion of background at an exposure of 1 ton-yr. The maximum sensitivity at lower Δm^2_{41} (< 1.0 eV^2) is observed when measurements are done at the PFBR reactor facility. In the mass region of $1.5 \leq \Delta m^2_{41}$ (eV^2) ≤ 6.0, sensitivities are comparable for all the reactors. Figure 3(b) shows the detector sensitivity with the inclusion of background assuming a signal (S) to background (B) ratio of 1. A combination of backgrounds is considered [45], such as a $1/E^2$ dependence that represents the spectral shape due to accidental backgrounds that arises from intrinsic detector radioactivity and a flat distribution in antineutrino energy due to contributions from fast neutrons. We have considered an associated 10% systematic uncertainty due to these backgrounds. It is observed that with the contribution of background, the active-sterile neutrino mixing angle sensitivity of the detector is further reduced. However, a small

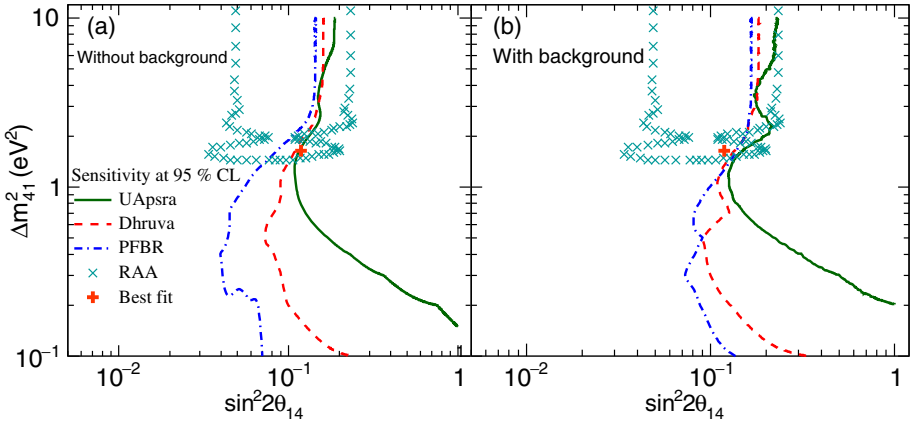

FIG. 3. The comparison of active-sterile neutrino mixing sensitivity for the ISMRAN setup placed at fixed distances of 4 m, 13 m, and 20 m from the U-Apsra, DHRUVA and PFBR reactors, respectively. The left (right) panel is without (with) inclusion of background in the simulated events. A signal to background ratio of 1 is considered.

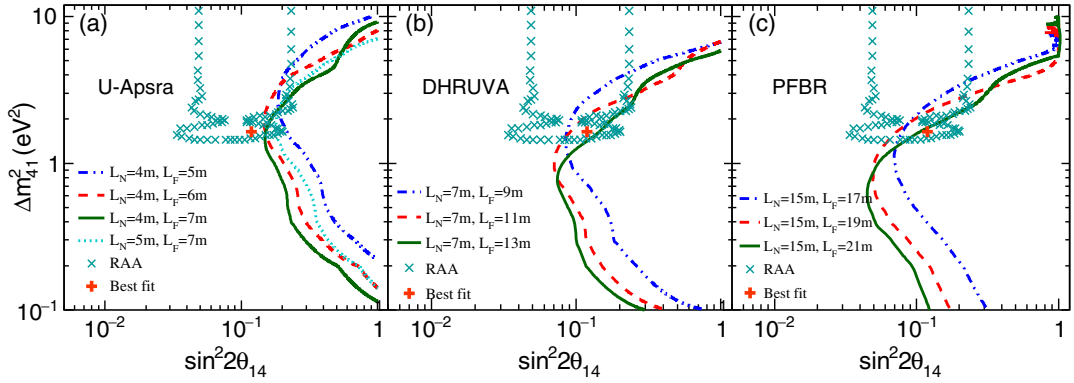

FIG. 4. The expected active-sterile neutrino mixing sensitivity of the ISMRAN setup in the $\sin^2\theta_{14} - \Delta m^2_{41}$ plane with a single detector which will be placed at a combination of near and far distances from the different reactor cores. The left, middle and, right panels represent results due to the U-Apsra, DHRUVA, and PFBR reactor facilities, respectively.

portion of the RAA region can be excluded using all the available neutrino sources, but the best-fit point as well as the remaining region of the RAA can be excluded with higher statistics, good detector energy resolution and with an improved signal to background ratio.

B. Detector at combination of distances

The discussions in the previous sub-section are based on a single detector placed at a fixed distance from the reactors. However, the systematic uncertainties due to reactor neutrino flux, as well as the detector play a major role when determining the active-sterile neutrino mixing sensitivity. In order to reduce the systematic uncertainties, we have considered combinations of near and far positions for the same detector from the reactor core for periods of six/twelve months at each location. For example, the detector can be placed at a near distance of 7 m from the DHRUVA reactor core for a period of six months and then at a far distance of 13 m for six months, for a total exposure of 1 ton-yr.

Figure 4 shows the ISMRAN setup sensitivity to active-sterile neutrino oscillation parameters in the $\sin^2 2\theta_{14} - \Delta m^2_{41}$ plane at 95% C.L. using several combinations of near and far detector positions from various reactor facilities, with an exposure of 1 ton-yr. A small portion of the RAA region can be excluded using $\bar{\nu}_e$s produced from three reactors. At lower Δm^2_{41} (< 1.0 eV^2), the detector sensitivity to the oscillation parameters is the best for the measurements carried out at the PFBR reactor. In the mass region of $1.0 \leq \Delta m^2_{41}$ (eV^2) ≤ 10.0, the detector can have the best sensitivity using $\bar{\nu}_e$s from U-Apsra reactor.[1] It can be noted that a power reactor has a longer burn-up period (more than 1 year). So there is a change in the reactor $\bar{\nu}_e$ flux with time. This can lead to reduction of the detector sensitivity to the active-sterile oscillation parameters if one is placing a single detector 6 months each at near and far position from the reactor core. In such a case, it is better to frequently change the position of the single detector and obtain a better sensitivity.

Further study has been performed in order to find out the effect of background considering the near and far sites of 7 m and 9 m from the DHRUVA reactor core. Similar types of background are considered as mentioned earlier for a single detector. In this case, we have assumed two different cases of background, $S/B = 1$ and 2. Figure 5 shows the comparison of the detector sensitivity between the ideal case and two scenarios with different S/B values. Due to the inclusion of backgrounds, the sensitivity of the

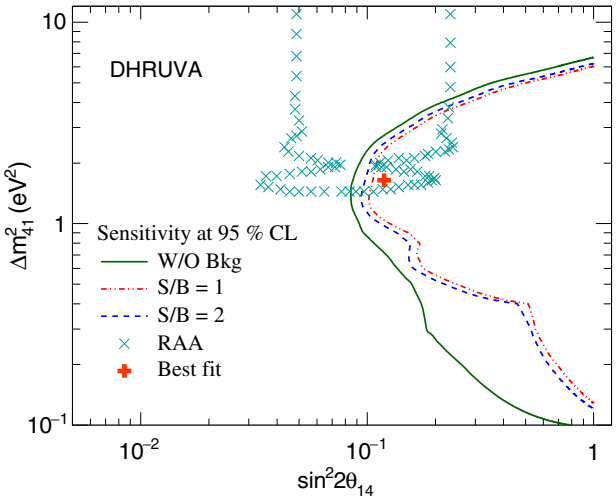

FIG. 5. Comparison of the ISMRAN sensitivity to the expected active-sterile neutrino mixing with and without inclusion of background for an exposure of 1 ton-yr. A single detector will be placed at a combination of near and far distances of 7 m and 9 m, respectively from the DHRUVA reactor.

[1]At a given near detector position, measurement of active-sterile neutrino oscillation parameters could be improved further by increasing the size of the far detector as mentioned in Ref. [45]. However, in the present study we have not considered the latter option.

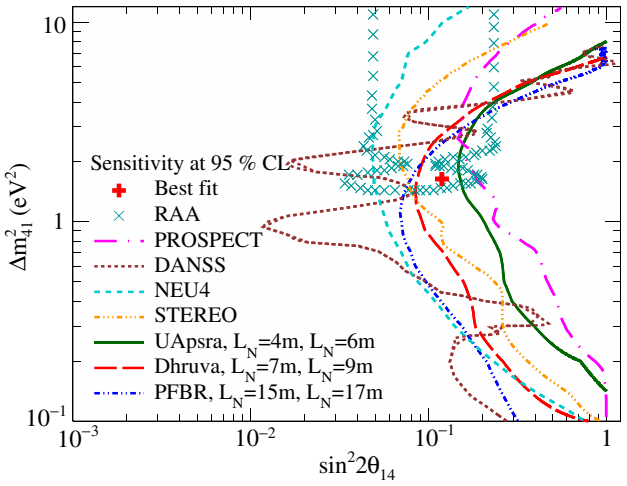

FIG. 6. The expected active-sterile neutrino mixing sensitivity of the ISMRAN setup in the $\sin^2 2\theta_{14} - \Delta m^2_{41}$ plane at 95% C.L. for an exposure of 1 ton-yr compared with other experimental observations. The detector is placed at a combination of near and far distances from the reactor different cores. NEU4 is the result from Neutrino-4 experiment.

detectors is reduced in the entire considered Δm^2_{41} range and a substantial reduction is observed for $\Delta m^2_{41} < 1.0$ eV^2. There is a small reduction of sensitivity in the RAA region by including the backgrounds.

Figure 6 shows the comparison between the expected sensitivity of the ISMRAN and other experimental observations such as PROSPECT [21], DANSS [19], STEREO [46], and Neutrino-4 [22] groups. As far as ISMRAN setup is concerned, the same detector will be placed at a combination of near and far positions from a given reactor core for a total exposure of 1 ton-yr. The sensitivity of the ISMRAN setup can be comparable with DANSS at $\Delta m^2_{41} = 0.1$ eV^2 if it will be placed at the near and far positions of 15 m and 17 m from the PFBR reactor core. It can be seen that at higher $\Delta m^2_{41} (> 1.0$ eV$^2)$, the sensitivity of the ISMRAN is comparable with the results from DANSS experiment, although Neutrino-4 experiment has better sensitivity as compared to all other mentioned observations. At low $\Delta m^2_{41} (< 0.2$ MeV$^2)$, ISMRAN sensitivity is comparable with Neutrino-4 observation if it will be placed at DHRUVA reactor facility. The present study shows that significant portions of the allowed RAA region can be excluded when the detector is placed at the near and far positions of 7 m and 9 m from the DHRUVA reactor core.

VIII. SUMMARY

The existence of sterile neutrinos as the possible origin of the RAA and the origin of the 5 MeV bump in the $\bar{\nu}_e$ energy spectra is being explored by several SBL experiments using reactor antineutrinos as a source. In the present study, we have investigated the potential of the upcoming ISMRAN experimental setup for finding out the possible presence of active to sterile neutrino oscillations. The analysis is performed for an exposure of 1 ton-year using $\bar{\nu}_e$s produced from the U-Apsra, DHRUVA, and PFBR reactor facilities, India. The oscillation parameters ($\sin^2 2\theta_{14}$, Δm^2_{41}) are constrained by considering a single detector which will be placed at either a fixed position or combining the observations taken at two different positions with respect to the reactor core. The main advantage of putting the same detector at different distances is to cancel the systematic uncertainties related to the reactor and detector. It is found that the ISMRAN setup can exclude a small portion of the favored nonzero active-sterile mixing parameters region obtained from RAA with a single detector placed at a fixed position. A combination of detector positions can have better sensitivity in excluding the RAA region as well as the best fit point compared to a detector placed at fixed location, for a given exposure. One of the possible combinations of near and far positions for the detector is 7 m and 9 m from the DHRUVA reactor core. This gave a better constraint of the RAA compared to other combinations. At lower Δm^2_{41} ($\sim$0.1 eV^2), the detector can have better sensitivity to the active-sterile oscillation parameters, if we place it at the PFBR reactor facility with a combination of near and far positions of 15 m and 17 m, respectively, from the core, due to its relatively compact core size and large thermal power. The sensitivity of the detector could be improved further with increased statistics by placing the target volume closer to the reactor and improving the signal to background ratios.

ACKNOWLEDGMENTS

We thank Anushree Ghosh for helpful suggestions and useful discussions. We also thank ISMRAN group members for useful discussion. We thank P. Garg and K. Finnelli for critically reading the manuscript. We would also like to take this opportunity to thank the anonymous referee for the valuable comments which helped us to improve the scope and content of the paper.

[1] F. Reines and C. L. Cowan, Phys. Rev. **92**, 830 (1953).
[2] Y. Abe *et al.* (Double Chooz Collaboration), Phys. Rev. Lett. **108**, 131801 (2012).
[3] F. An *et al.* (Daya Bay Collaboration), Phys. Rev. Lett. **108**, 171803 (2012).
[4] J. Ahn *et al.* (RENO Collaboration), Phys. Rev. Lett. **108**, 191802 (2012).
[5] T. A. Mueller *et al.*, Phys. Rev. C **83**, 054615 (2011).
[6] P. Huber, Phys. Rev. C **84**, 024617 (2011).
[7] G. Mention, M. Fechner, T. Lasserre, T. A. Mueller, D. Lhuillier, M. Cribier, and A. Letourneau, Phys. Rev. D **83**, 073006 (2011).
[8] F. von Feilitzsch, A. A. Hahn, and K. Schreckenbach, Phys. Lett. **118B**, 162 (1982).
[9] K. Schreckenbach, G. Colvin, W. Gelltely, and F. von Feilitzsch, Phys. Lett. **160B**, 325 (1985).
[10] A. A. Hahn, K. Schreckenbach, W. Gelletly, F. von Feilitzsch, G. Colvin, and B. Krusche, Phys. Lett. B **218**, 365 (1989).
[11] A. C. Hayes and P. Vogel, Annu. Rev. Nucl. Part. Sci. **66**, 219 (2016).
[12] P. Huber, Nucl. Phys. **B908**, 268 (2016).
[13] Y. Abe *et al.* (Double Chooz Collaboration), J. High Energy Phys. 01 (2016) 163.
[14] F. P. An *et al.* (Daya Bay Collaboration), Phys. Rev. Lett. **116**, 061801 (2016).
[15] J. H. Choi *et al.* (RENO Collaboration), Phys. Rev. Lett. **116**, 211801 (2016).
[16] Y. J. Ko *et al.*, Phys. Rev. Lett. **118**, 121802 (2017).
[17] F. An *et al.* (Daya Bay Collaboration), Phys. Rev. Lett. **118**, 251801 (2017).
[18] S. Boser, C. Buck, C. Giunti, J. Lesgourgues, L. Ludhova, S. Mertens, A. Schukraft, and M. Wurm, Prog. Part. Nucl. Phys. **111**, 103736 (2020).
[19] I. Alekseev *et al.* (DANSS Collaboration), Phys. Lett. B **787**, 56 (2018).
[20] H. Almazn *et al.* (STEREO Collaboration), Phys. Rev. Lett. **121**, 161801 (2018).
[21] J. Ashenfelter *et al.* (PROSPECT Collaboration), Phys. Rev. Lett. **121**, 251802 (2018).
[22] A. P. Serebrov *et al.* (NEUTRINO-4 Collaboration), Pis'ma Zh. Eksp. Teor. Fiz. **109**, 209 (2019) [JETP Lett. **109**, 213 (2019)].
[23] S. Gariazzo, C. Giunti, M. Laveder, and Y. F. Li, J. High Energy Phys. 06 (2017) 135.
[24] S. P. Behera, D. K. Mishra, and L. M. Pant, Eur. Phys. J. C **79**, 86 (2019).
[25] D. Mulmule, S. P. Behera, P. K. Netrakanti, D. K. Mishra, V. K. S. Kashyap, V. Jha, L. M. Pant, B. K. Nayak, and A. Saxena, Nucl. Instrum. Methods Phys. Res., Sect. A **911**, 104 (2018).
[26] S. K. Agarwal, C. G. Karhadkar, A. K. Zope, and K. Singh, Nucl. Eng. Des. **236**, 747 (2006).
[27] T. Singh, P. Pandey, T. Mazumdar, K. Singh, and V. K. Raina, Ann. Nucl. Energy **60**, 141 (2013).
[28] S. C. Chetal, V. Balasubramaniyan, P. Chellapandi, P. Mohanakrishnan, P. Puthiyavinayagam, C. P. Pillai, S. Raghupathy, T. K. Shanmugham, and C. Sivathanu Pillai, Nucl. Eng. Des. **236**, 852 (2006).
[29] S. Oguri, Y. Kuroda, Y. Kato, R. Nakata, Y. Inoue, C. Ito, and M. Minowa, Nucl. Instrum. Methods Phys. Res., Sect. A **757**, 33 (2014).
[30] Z. Maki, M. Nakagawa, and S. Sakata, Prog. Theor. Phys. **28**, 870 (1962).
[31] M. C. Gonzalez-Garcia and Y. Nir, Rev. Mod. Phys. **75**, 345 (2003).
[32] T. Kajita and Y. Totsuka, Rev. Mod. Phys. **73**, 85 (2001).
[33] C. Bemporad, G. Gratta, and P. Vogel, Rev. Mod. Phys. **74**, 297 (2002).
[34] P. F. de Salas, D. V. Forero, C. A. Ternes, M. Tortola, and J. W. F. Valle, Phys. Lett. B **782**, 633 (2018).
[35] A. Palazzo, J. High Energy Phys. 10 (2013) 172.
[36] S. Gariazzo, C. Giunti, M. Laveder, and Y. F. Li, Phys. Lett. B **782**, 13 (2018).
[37] M. Dentler, Á. Hernndez-Cabezudo, J. Kopp, P. A. N. Machado, M. Maltoni, I. Martinez-Soler, and T. Schwetz, J. High Energy Phys. 08 (2018) 010.
[38] L. Zhan, Y. Wang, J. Cao, and L. Wen, Phys. Rev. D **78**, 111103 (2008).
[39] P. Huber, Nucl. Phys. **B908**, 268 (2016).
[40] *Nuclear Reactor Engineering*, edited by S. Glasstone and A. Sesonske (Von-Nostrand, Princeton, 1994).
[41] P. Vogel and J. F. Beacom, Phys. Rev. D **60**, 053003 (1999).
[42] M. C. Gonzalez-Garcia and M. Maltoni, Phys. Rev. D **70**, 033010 (2004).
[43] P. Huber, M. Lindner, T. Schwetz, and W. Winter, Nucl. Phys. **B665**, 487 (2003).
[44] S. H. Seo *et al.* (RENO Collaboration), Phys. Rev. D **98**, 012002 (2018).
[45] K. M. Heeger, B. R. Littlejohn, H. P. Mumm, and M. N. Tobin, Phys. Rev. D **87**, 073008 (2013).
[46] H. Almazn Molina *et al.* (STEREO Collaboration), arXiv: 1912.06582.